SYNTHESIS, CHARACTERIZATION, AND NMR STUDY OF OXO-CENTERED TRINUCLEAR COMPLEXES $[Fe_2^{III}Ni^{II}O(O_2CC_2H_5)_6(py)_3]\cdot py$ and $[Fe_2^{III}Ni^{II}O(O_2CC_2H_5)_6(H_2O)_3]\cdot H_2O$[**]

Xin Wang[*], Zhiwei Chen, Yingyang Lv, Shuhui Cai, Zhong Chen

Xiamen University, Xiamen 361005, China; e-mail: wx@xmu.edu.cn

Two μ_3-oxo carboxylate-bridged heteronuclear complexes, $[Fe_2^{III}Ni^{II}O(O_2CC_2H_5)_6(H_2O)_3]\cdot H_2O$ and $[Fe_2^{III}Ni^{II}O(O_2CC_2H_5)_6(py)_3]\cdot py$, were prepared and characterized by several spectroscopic techniques including NMR, X-ray diffraction, IR, ESR, and UV. X-ray diffraction measurements demonstrated that the Fe_2NiO clusters of the complexes were close to threefold symmetry in crystals. The ligands coordinated to different metal atoms were almost equivalent in the IR timescale but in equivalent in the NMR timescale. The NMR results showed that the largest ^1H NMR chemical shift of the complex was 95.1 ppm, implying its paramagnetic property, which was weakened by the antiferromagnetic interaction of metal ions through the μ_3-O bridge. NMR and IR studies indicated that the complexes were stable in various nonpolar and moderately polar solvents, such as $CDCl_3$ and d_3-MeCN, but they were decomposed into metal ions and the corresponding ligands in strong polar solvents, such as water, at room temperature. Assignments of the ^1H NMR spectra of the complexes were made on the basis of relative intensities, broadening, variable temperature experiments, spin-lattice relaxation times, and substitution by appropriate ligands. The ^1H spin-lattice relaxation time T_1 and variable-temperature NMR experiments were also applied to investigate the solution structures and dynamics of the complexes. It is worth noting that the ^1H chemical shift of the pyridine coordinated to the metals could be greater than 90 ppm.

Keywords: *nuclear magnetic resonance, trinuclear complexes, oxo-centered complexes, carboxylate complexes.*

СИНТЕЗ, ХАРАКТЕРИСТИКИ И ИССЛЕДОВАНИЕ МЕТОДОМ ЯМР ОКСОЦЕНТРИРОВАННЫХ ТРЕХЪЯДЕРНЫХ СОЕДИНЕНИЙ $[Fe_2^{III}Ni^{II}O(O_2CC_2H_5)_6(py)_3]\cdot py$ и $[Fe_2^{III}Ni^{II}O(O_2CC_2H_5)_6(H_2O)_3]\cdot H_2O$

X. Wang[*], Zh.-W. Chen, Y. Lv, Sh. Cai, Zh. Chen[*]

УДК 539.143.43

Сямэньский университет, Сямынь 361005, Китай; e-mail: wx@xmu.edu.cn

(Поступила 24 апреля 2018)

Получены и охарактеризованы несколькими спектроскопическими методами (ЯМР, рентгеновская дифракция, ИК, ЭПР и УФ) два гетероядерных карбоксилатных комплекса с μ_3-оксомостиками: $[Fe_2^{III}Ni^{II}O(O_2CC_2H_5)_6(H_2O)_3]\cdot H_2O$ и $[Fe_2^{III}Ni^{II}O(O_2CC_2H_5)_6(py)_3]\cdot py$. Рентгеноструктурные измерения показывают, что кластеры Fe_2NiO комплексов обладают симметрией, близкой к кристаллической симметрии класса 3. Для лигандов, координированных с различными металлами, обнаружена практически эквивалентность ИК спектров, но не эквивалентность спектров ЯМР. Результаты ЯМР показывают наибольший химический сдвиг ^1H 95.1 м.д., что указывает на парамагнетизм комплекса, который ослаблен антиферромагнитным взаимодействием ионов металлов через мостик μ_3-O. Согласно результатам ЯМР и ИК исследований, комплексы стабильны в различных неполярных и умеренно полярных растворителях, таких как $CDCl_3$ и d_3-MeCN, но разлагаются на ионы металлов и соответствующие лиганды в сильных полярных растворителях, таких как вода, при комнатной

[**] Full text is published in JAS V. 86, No. 3 (http://springer.com/10812) and in electronic version of ZhPS V. 86, No. 3 (http://www.elibrary.ru/title_about.asp?id=7318; sales@elibrary.ru).

температуре. Сопоставление в ^{1}H ЯМР спектрах проводилось на основе анализа относительных интенсивностей, уширения, экспериментов при различных температурах, времен спин-решеточной релаксации и замещения соответствующими лигандами. Эксперименты по спин-решеточной релаксации ^{1}H и измерения методом ЯМР при переменной температуре осуществлялись также для исследования структур растворов и динамики комплексов. Химический сдвиг ^{1}H для пиридина, скоординированного с металлами, может превышать 90 м.д.

Ключевые слова: *ядерный магнитный резонанс, трехъядерные комплексы, оксоцентрированные комплексы, карбоксилатные комплексы.*

Introduction. Investigation of the properties of mixed-metal and mixed-valence complexes is important for understanding the dynamics of the electron transfer process [1–3]. The family of metal complexes with the general formula $[M_xM'_{3-x}(\mu_3\text{-}O)(\mu\text{-}O_2CR)_6L_3]^{n+}$ (M, M' = V, Cr, Mn, Fe, Co, Ni, Ru, Rh, Ir; x = 1, 2, 3; n = 0, 1, 2, 4, 7; O_2CR = fatty acid, substituted fatty acid or amino acid group; L = H_2O, C_5H_5N, or Ph_3P) is of particular interest [1–11]. Among the main problems one should note antiferromagnetic coupling in mixed-metal clusters [1, 2, 4–7] and electron delocalization in mixed-valence clusters [1, 8–13] when their symmetries are lowered. It is shown that the structure of mixed-metal or mixed-valence pivalate-bridged complexes in CD_2Cl_2 or $CDCl_3$ is the same as that in the solid state. Ligand exchange is slow for carboxylate groups but much faster for terminal pyridines [10, 11, 14]. How about the title complexes? Do they possess the same properties? Do different solvents influence their properties?

Paramagnetic systems are characterized by short relaxation times and large chemical shifts due to the magnetic coupling of nuclear spins with unpaired electrons [15]. In general, 2D NMR experiments require the application of two or more pulses interleaved by variable and fixed delays to allow the development of coherence. After each pulse the spin system may relax back to equilibrium before magnetization or coherence has been transferred between different sets of spins. As a result, the intensities of the cross peaks are predicted to be much smaller than those for slow-relaxing systems. Although many papers have been published to interpret various spectroscopic properties of mixed-metal trinuclear carboxylate complexes, a few studies on their NMR spectroscopy have been reported [10, 16]. Most reports about NMR to date have been limited to homonuclear $[M_3O(OOCR)_6L_3]^{n+}$ complexes [11, 14, 17–21]. For more complicated cases, such as oxo-centered mixed-valence heterotrinuclear transition-metal complexes, however, there are few NMR studies, presumably because of the difficulty in the assignment of NMR resonances with broad peaks and the uncertainty in proton-proton connectivity. However, NMR spectroscopy may provide information on the magnetic and electronic properties of the metal centers, as well as on the nature and extent of metal-ligand covalency [22, 23].

In this paper, we demonstrated the feasibility to apply some important NMR techniques, such as proton longitudinal relaxation time, in aiding the NMR signal assignment and determination of the solution structures and the dynamics of the title complexes. Our results confirmed that the crystal structures of the complexes could quite satisfactorily explain their solution structures in d_6-DMSO, d_3-MeCN, and $CDCl_3$ solvents. While in water, the complexes decompose into metal ions and corresponding ligands at room temperature.

Experimental. All materials are reagent grade. Reagents were obtained from commercial sources and used as received. Analyses for carbon, hydrogen, and nitrogen were performed on a Vario-Elmar III elemental analyzer, and Fe and Ni were determined using a DRC e ICP-MS.

Preparation of complexes[$Fe_2^{III}Ni^{II}O(O_2CC_2H_5)_6(H_2O)_3]\cdot H_2O$ (labeled as [Fe_2NiOPH]). $NiCl_2\cdot 6H_2O$ (2.38 g, 0.01 mol) and $NaOOCC_2H_5$ (9.6 g, 0.1 mol) were mixed after being dissolved in water separately. The solution with 3.24 g of $FeCl_3$ (0.02 mol) and 50 mL of H_2O was slowly added with stirring to the above-mentioned mixture at 70°C. After 3 h of refluxing, the obtained brown-green crystals were filtered, washed copiously with ethanol, and finally dried in open air (yield 90%). Anal. calcd for $Fe_2NiO_{17}C_{18}H_{38}$ (%): Fe, 16.1; Ni, 8.5; C, 31.0; H, 5.5. Found (%): Fe, 16.3; Ni, 8.2; C, 30.8; H, 5.2.

Preparation of complexes [$Fe_2^{III}Ni^{II}O(O_2CC_2H_5)_6(py)_3]\cdot py$ (labeled as [Fe_2NiOPP]). The above-prepared product (1 g) was dissolved in hot pyridine (10 mL). The solution was stirred for 30 min, then filtrated and cooled to 4°C. Several days later, the solution gave black-red crystals. Filtering and washing the solid with pyridine gave the product (yield 42.8%). Anal. calcd. for $Fe_2NiO_{13}N_4C_{38}H_{50}$ (%): Fe, 11.9; Ni, 6.3; C, 48.6; H, 5.3; N, 6.0. Found (%): Fe, 12.1; Ni, 6.5; C, 48.0; H, 5.6; N, 5.8.

Crystal structures were determined on a Bruker Smart APEX CCD diffractometer using graphite-monochromated MoK_α (0.71073 Å) radiation. Data were collected in the range of $0 \le 2\theta \le 50°$ at 0°C. Crystallographic data for [Fe_2NiOPP] are listed in Table 1. The intensities were corrected for Lorentz and polarization

effects, and an empirical absorption correction based on PSI and DIFABS scan data was performed. A structural solution was accomplished with the program TAXSAN. All non-hydrogen atoms were refined with anisotropic thermal parameters by the full-matrix least-square to final R_w. Hydrogen atoms were placed at calculated positions.

TABLE 1. Crystal data and details of X-ray experiment for [Fe_2NiOPP]

Empirical formula	$Fe_2NiO_{13}N_4C_{38}H_{50}$	Z	4
Formula weight	939.38	$F(000)$	978
Crystal system	Triclinic	D_{calc}, g/cm^3	1.383
Space group	P-1	T (K)	273(2)
a, Å	12.669(6)	Radiation, Å	MoK_α, 0.71073
b, Å	12.690(8)	Scan mode	ω–2θ
c, Å	17.394(8)	$2\theta_{max}$, degree	50
α, degree	71.643(14)	$I \geq 3\sigma(I)$	1067
β, degree	71.275(9)	R_w[a]	0.0983
γ, degree	60.151(9)	R_w[b]	0.1557
V, Å^3	2256(2)		

IR spectra were obtained using KBr disks on a Nicolet SX-740 FTIR spectrometer and a Digilab FTS20E/D-V spectrometer. Electronic spectra were recorded using a Shimudzu Model UV-3000 UV-VIS double-wavelength spectrophotometer. ESR spectra were recorded using a Bruker ER 200D-SRCESR spectrophotometer.

NMR spectra were obtained using a Varian NMR System 500 spectrometer. Chemical shifts were reported on the δ scale (shifts downfield are positive) using TMS as a reference. Due to the possible large range of ^{1}H chemical shifts, the 100 kHz spectrum width was used in all 1D experiments. In order to excite the spin systems uniformly in the whole spectrum width, a 2 μs (≈20° in the flip angle) pulse was applied. This warranted the validity of integration for all non-overlapped peaks; 64 K data points, 1.0 s repetition time, and 128 transients were adopted for 1D ^{1}H spectra. Signal-to-noise ratios were improved by a line-broadening factor of 3 Hz in Fourier transformation for all 1D spectra; T_1 measurements were performed using a standard inversion-recovery sequence (180°-τ-90°-Acq) to obtain non-selective proton longitudinal relaxation times.

Results and discussion. *Structure description.* Although the molecules occupy general sites and thus have no internal symmetry, the central Fe_2NiO cluster is fairly close to threefold symmetry. The central oxygen almost locates in the plane of the three metal atoms, and all the metal atoms show similar coordination. Table 2 lists some selected bond lengths and angles for [Fe_2NiOPP]. Like heteronuclear acetate complexes [4, 24], the difference between M-μ_3O distances is only 0.02 Å, as in the case of the homonuclear $Fe_3^{III}O$ complex [9]. The patterns of coordination to the carboxylate oxygens are also similar to each other. Because there is no definite evidence for the localization of the Ni^{2+} ion, we assume that three metal atoms are distributed randomly. The three MO_4 planes are nearly at right angles to that of the central Fe_2NiO cluster. As the distance between the coordinated terminal pyridine nitrogen atom and the metal ion is longer than

TABLE 2. Selected bond lengths and bond angles for [Fe_2NiOPP]

Bond distances, Å				Bond angles, degree			
M_1–O	1.881	M_3–O_{34}	2.043	O–M_3–O_{33}	94.59	O–M_2–O_{31}	97.12
M_2–O	1.896	M_1–O_{22}	2.018	O–M_3–O_{23}	96.73	O–M_2–O_{13}	95.36
M_3–O	1.904	M_1–O_{21}	2.041	O–M_3–O_{24}	95.46	O–M_2–O_{14}	95.02
M_3–N_3	2.199	M_1–O_{12}	2.033	O–M_3–O_{34}	96.55	O–M_2–O_{32}	97.0
M_1–N_1	2.208	M_1–O_{11}	2.052	O–M_1–O_{22}	95.44	M_2–O–M_1	120.02
M_2–N_2	2.191	M_2–O_{31}	2.036	O–M_1–O_{21}	94.45	M_2–O–M_3	119.37
M_3–O_{33}	2.038	M_2–O_{13}	2.040	O–M_1–O_{12}	97.34	M_1–O–M_3	120.61
M_3–O_{23}	2.040	M_2–O_{14}	2.060	O–M_1–O_{11}	97.54		
M_3–O_{24}	2.040	M_2–O_{32}	2.049				

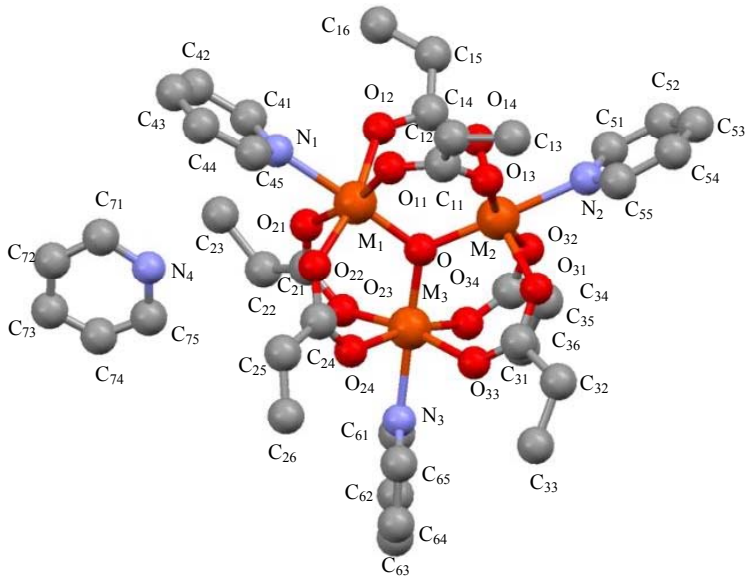

Fig. 1. Molecular structure of [Fe_2NiOPP] (hydrogen atoms are removed for clarity).

that between the metal ion and the central oxygen, the coordination of the metal centers is slightly distorted octahedral. The molecular structure of [Fe_2NiOPP] is shown in Fig. 1.

Infrared spectroscopy. The selected IR data of the title complexes and some related compounds are given in Table 3. Most of the bands due to the vibrations of the title complexes were identified by comparison with free pyridine, and sodium propionate, as discussed in [5, 25, 26]. The bands arising from the pyridine ligand are not discussed here as there are only slight changes from free pyridine. The OCO bands between 400 and 800 cm^{-1} are listed for comparison with acetate complexes in [25, 26]. For the bands higher than 800 cm^{-1}, which are not discussed in [25, 26], compared with sodium propionate, the observed vibrational frequencies $\upsilon_{as}(CO_2)$ and $\upsilon_s(CO_2)$ for the propionate ligands of the complexes move to higher frequencies. For the two mixed-metal complexes, the data of the propionate stretching frequencies indicate that all six propionates are approximately equivalent and best represented as bidentate bridges. This is in agreement with the X-ray analysis results. Compared to the homonuclear Fe_3O complex, the introduction of the Ni atom causes a small change in the vibrational frequencies of the bridging propionates in heteronuclear Fe_2NiO complexes [25].

TABLE 3. Selected IR bands (cm^{-1}) for the title and related compounds

Compound	$\upsilon_{as}(CO_2)$	$\upsilon_s(CO_2)$	δ_{OCO}	π_{OCO}	ρ_{rOCO}	$\upsilon_{as}(Fe_2MO)$
[Fe_2NiOPH]	1597	1423	672	640	463	722, 575
[Fe_2NiOPP]	1630	1416	659	630	465	710, 567
[Fe_2NiOPP] [a]	1627	1415	657	631	464	711, 565
[Fe_3OPH][b]	1572	1431	680	646	527	596
[Fe_2NiOAH][c]			665	620	540	730, 580
[Fe_2NiOAP][c]			658	620	535	722, 565
$NaOOCC_2H_5$	1570	1410		640	500	

[a] [Fe_2NiOPP] refers to [Fe_2NiOPP] chloroform solution.
[b] [Fe_3OPH] refers to [$Fe_3O(OOCC_2H_5)_6{\cdot}(H_2O)_3$]$Cl{\cdot}3H_2O$.
[c] Refer to [25], A = acetate.

In trinuclear Fe_3^{III} complexes, $\upsilon_{as}(Fe_3O)$ belongs to the E' symmetry due to the D_{3h} symmetry of the Fe_3O core. According to the assignment of [10, 25, 27], the $\upsilon_{as}(Fe\text{-}\mu_3O)$ band is around 630 cm^{-1} for $Fe_3^{III}O$ complexes. Therefore, the 596 cm^{-1} band of [Fe_3OPH] is readily assigned to $\upsilon_{as}(Fe_3O)$. When one Fe^{III} ion is replaced by one Ni^{II} ion, this band splits into two bands, as in the case of mixed-valence and mixed-metal $Fe_2^{III}M^{II}$ complexes due to the symmetry reduction [9, 10, 25]. The results are in good agreement with the

corresponding data of acetate complexes [25]. There is only a slight change in the $\upsilon_{as}(Fe_2MO)$ when pyridine terminal ligands are exchanged by H_2O.

When the [Fe_2NiOPP] crystal was dissolved in a $CHCl_3$ solvent, the observed vibrational frequencies $\upsilon_{as}(Fe\text{-}\mu_3O)$ and $\upsilon_s(Ni\text{-}\mu_3O)$ of the liquid complexes were almost the same as those of solid[Fe_2NiOPP]. But if the [Fe_2NiOPP] crystal was dissolved in an H_2O solvent, there was no observed vibrational frequencies $\upsilon_{as}(Fe\text{-}\mu_3O)$ or $\upsilon_s(Ni\text{-}\mu_3O)$ anymore. Therefore, the crystal is stable in various nonpolar solvents, but it is decomposed in strong polar solvents at room temperature. This conclusion can be clearly seen from IR spectra in Fig. 2.

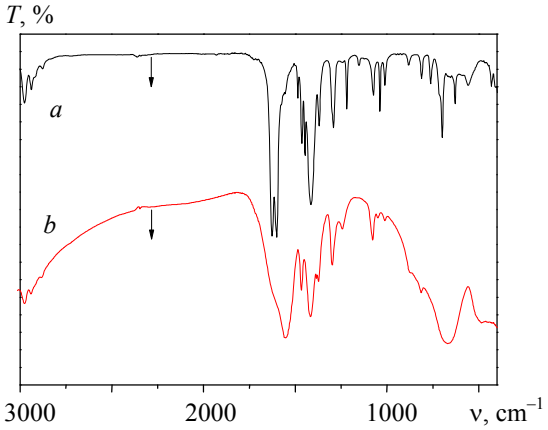

Fig. 2. IR spectroscopy for [Fe_2NiOPP] dissolved in H_2O (a) and $CHCl_3$ solvents (b).

UV spectroscopy. UV experiments were carried out in H_2O. For the [Fe_2NiOPP] aqueous solution, there are a strong absorption peak at 255 nm and a sharp peak at 208 nm. For the [Fe_2NiOPH] aqueous solution, one sharp peak occurs at 205 nm. Compared with the UV spectra of pyridine (255 nm) and sodium propionate (208 nm) aqueous solutions, it is easy to assign the peak at 255 nm to π–π^* electron transition on the dissociative pyridine ring, and the peaks at 208 and 205 nm to π–π^* electron transition on the carboxyl of propionate. These results indicate the decomposition behavior of the title complexes in H_2O.This is an interesting phenomenon because both of them were generally considered to be stable in aqueous solutions, especially for [Fe_2NiOPH] which was prepared directly from an aqueous solution.

ESR spectroscopy. There were no differences in the two ESR spectra in Fig. 3; one was tested for a blank tube, another was tested for a [Fe_2NiOPP] chloroform solution in the tube. So there was almost no ESR signal, neither for the room temperature nor for the lower temperature for the sample complex. We think that the main reason is in the following. The Ni^{2+} ion has a large orbital angular momentum as a result of the ground state energy level being 3F, so the component of this orbital angular momentum can mix with the ground state through spin-orbit coupling to make some contribution to the ground state of the cluster

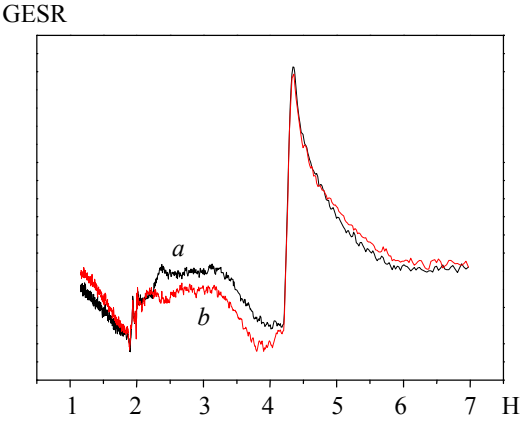

Fig. 3. ESR spectroscopy for the blank tube (a) and the [Fe_2NiOPP] chloroform solution in the tube (b).

with the orbital angular momentum components. The delocalization of the outermost electrons of the Ni^{2+} ion become to larger by exchanging with Fe^{3+} ions through the oxo-O atom, and the large orbital angular momentum has strong interaction with the crystal lattice, and the spin-lattice relaxation time may be short and the spectral peaks wide, and therefore the ESR signal of the complex cannot been observed.

NMR spectroscopy. Due to paramagnetic broadening, no *J* splitting was resolved for any ^1H NMR signal. Selective proton decoupling measurements showed very small effects on the line width, typically a narrowing of several Hz. Therefore, the assignment of the ^1H NMR of the complexes was carried out based on their relative intensities, broadening, variable temperature experiments, longitudinal relaxation time, and substitution of the appropriate ligands. For comparison, we first measured the ^1H NMR of two oxo-centered carboxylate-bridged tri-iron complexes $[Fe_3^{III}O(O_2CC_2H_5)_6(H_2O)_3]Cl\cdot 3H_2O$ (labeled as [Fe_3OPH]) and $[Fe_3^{III}O(O_2CC_2H_5)_6(py)_3]ClO_4\cdot 3H_2O$ (labeled as [Fe_3OPP]). Both complexes were prepared according to the method of Chen et al. [28]. [Fe_3OPH] gives two resonances at 25.8 and 7.4 ppm besides the signal from the residual free water. The terminal water ligands are very close to the iron ions (separated by one oxygen only in the σ-bonding framework). Owing to this, the resonances of protons in the terminal waters cannot be observed. Thus two peaks are easily assigned to the $–CH_2$ and $–CH_3$ groups on the bridging propionate ligands, respectively, by comparing their relative integral intensities. Based on this assignment, the two resonances in the spectrum of [Fe_3OPP] at 25.4 and 7.5 ppm are readily assigned to $–CH_2$ and $–CH_3$ protons. This agrees with the results of 25.1 and 7.6 ppm when the terminal ligands are N-methylimidazole [21], indicating the small effect of the terminal ligands. The remaining three resonances of [Fe_3OPP] must arise from pyridine ligands. The resonance at 8.3 ppm is assigned to the 4-position proton (4-H) according to its relative intensity. Because the 3-H of pyridine ligands is farther from ferric ion than the 2-H, the sharper signal at 29.0 ppm is assigned to the 3-H, leaving the broader one at 65.0 ppm to the 2-H. These values are close to the results previously reported for a similar acetate-bridging complex [18]. In [Fe_3OPP], all three pyridine resonances are downfield, with the magnitude of shifts in the order of 2-H > 3-H > 4-H as expected for a predominant through bond (contact) mechanism [10, 11, 18].

Unlike the complexes [Fe_3OPH] and [Fe_3OPP] [20], the complexes [Fe_2NiOPH] and [Fe_2NiOPP] do not have threefold symmetry. Consequently, their ^1H NMR spectra may exhibit twice as many peaks as those of the corresponding Fe_3O complexes. Recently, Wu et al. [9] reported a ^1H NMR study of electron transfer between $[Fe_3^{III}O(O_2CC_2H_5)_6(py)_3]^+$ and $[Fe_3^{III}Fe^{II}O(O_2CC_2H_5)_6(py)_3]^0$. However, as the samples they used are mixtures of heteronuclear and homonuclear species, no detailed information has been given. In our case, excluding residual solvent peaks, [Fe_2NiOPH] and [Fe_2NiOPP] are expected to give four and ten ^1H resonances, respectively, in the ideal case. The variable-temperature ^1H NMR spectra of [Fe_2NiOPP] in d_3-MeCN are shown in Fig. 4. The peak at 2.6 ppm is contributed by the residual proton of the solvent and

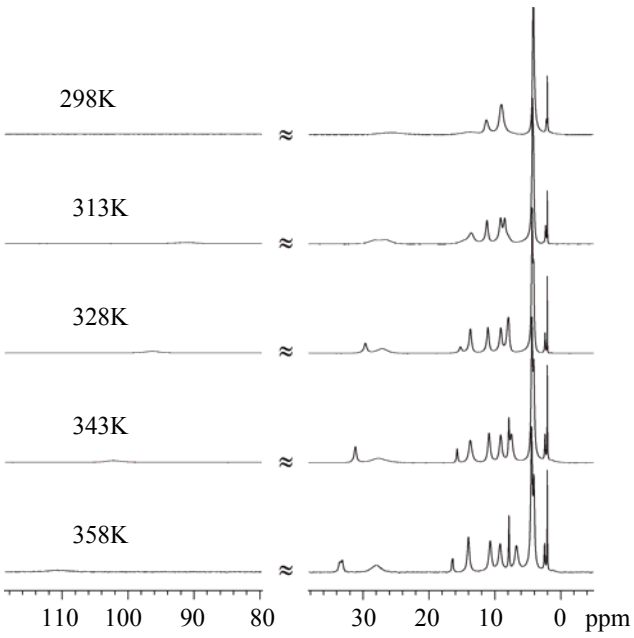

Fig. 4. Variable-temperature ^1H NMR spectra of [Fe_2NiOPP] in d_3-MeCN.

the peak at 3.4 ppm comes from the residual free water. Similar to [Fe_3OPH] [18, 20], the proton peak of the terminal water ligands is broadened beyond detection because of their proximity to the metal centers. The area ratio of the signal at 4.9 to 3.8 ppm is 2:1. The same ratio exists between the signals at 10.6–10.8 and 9.7 ppm. Moreover, the area ratio of the upfield signals (4.4 ± 0.6 ppm) to downfield signals (10.5 ± 1 ppm) is 3:2. Therefore, the least intense signals (10.5 ± 1 ppm) with a greater downfield shift are assigned to the methylene protons of the bridging propionate ligands. This is in line with their closer proximity to the metal centers. The assignment of all the four resonances of [Fe_2NiOPH] is listed in Table 4. Obviously, all proton chemical shifts are moved to downfield when one of Fe^{3+} ions is replaced by a Ni^{2+} ion. Unlike IR spectra, the propionate ligands that bridge the Fe-Fe pair are no longer equivalent to those bridge Fe–Ni pairs in the NMR timescale.

Fortunately, only ten ^1H resonances are observed for [Fe_2NiOPP] in the deutero-acetone solvent. They are divided into two groups with an intensity ratio of 2:1, as the pyridine ligands are nonequivalent as well as propionate ligands. Due to broad resonances and short T_2, only $–CH_2$ and $–CH_3$ peaks of the bridging propionate ligands are easily discriminated. There are slight differences in the ^1H chemical shifts of the bridging propionate ligands between [Fe_2NiOPH] and [Fe_2NiOPP] (see Table 4). The remaining six resonances come from the pyridine ligands. It is difficult to assign them unambiguously. Although White and co-workers showed the ^1H NMR spectra of [$Fe_2MO(OOCCMe_3)_6py_3$] (M = Ni, Co) in $CDCl_3$ [10], no assignment of the peaks from pyridine has been reported. Using complexes with different deuterium-labeled ligands may simplify the NMR spectra and help achieve unambiguous assignment [18], but it is arduous work. Because longitudinal relaxation time T_1 contains both structural and dynamic information [15], it may provide information on the mobility of protons and hence assist assignment [23]. Therefore, the longitudinal relaxation times of all signals of [Fe_2NiOPP] were measured in order to confirm the assignment of peaks from nonequivalent pyridine ligands. They range from 0.7 to 5.9 ms (Table 4), which are much shorter than the corresponding values in diamagnetic systems.

Although there are three principal types of magnetic interactions related to the spin-lattice relaxation of spin $I = 1/2$ nuclei, the most important one in paramagnetic systems is dipole-dipole interaction. The nucleus experiences a fluctuating field due to the motion of neighboring magnetic dipoles coming from unpaired electrons or other nuclei. The field arising from a dipole moment of strength μ at a distance r and subtending an angle θ with respect to the direction of static magnetic field B_0 is given by the simple formula [15]

$$B_{DD} = \pm\mu_0\mu(3\cos^2\theta - 1)/4\pi r^3.$$

The larger the B_{DD}, the stronger the dipole-dipole interaction and the shorter longitudinal relaxation time. Assuming that μ and θ are the same, the distances of pyridine protons to the transition-metal atoms are 2-H < 3-H < 4-H, so their longitudinal relaxation times should change according to the sequence 2-H < < 3-H < 4-H. This is proved by the experimental results. The relaxation time of the 2-H of pyridine (~0.8 ms) is significantly shorter than that of the 3-H (3.5–3.7 ms). It is interesting to note that the protons at the same site of pyridines coordinated by different metals in [Fe_2NiOPP] have almost the same longitudinal relaxation times. This demonstrates the usefulness of longitudinal relaxation time to provide the information that may be impossible to obtain from routine 1D experiment for complicated complexes. According to longitudinal relaxation times and relative intensities, the remaining six resonances of [Fe_2NiOPP] were assigned rationally (see Table 4). The chemical shift ratio of Ni-py, 2-H:3-H:4-H = 1:0.306:0.153, compared to 1:0.297:0.0664 of the mononuclear Ni-py complex [29], indicates the nonequivalent influence of the other group on Ni-py. Compared with the Fe_3O complex, the resonances of protons of pyridine coordinated by Fe ions shift upfield.

The chemical shifts and line widths can be affected by both through-bond (contact) and through-space (dipolar) mechanisms. Similar to the case with pivalate ligands [10], the unpaired electron density of the Ni^{2+} ion is delocalized onto pyridine to a greater extent than onto propionate ligands as there is a large π bond on pyridine. Consequently, the pyridine resonances are influenced more strongly than the propionate resonances, as shown by their greater chemical shifts and broader line widths. The NMR data reveal that the chemical shifts of the pyridines and methylene are predominantly due to the contact mechanism, while those of methyl are due to both contact and dipolar mechanisms [30]. Though Fe^{III} and Ni^{II} are paramagnetic, the antiferromagnetic interactions between the metal ions through the oxo-centered and the bridging propionate ligands weaken the influence of paramagnetism.

TABLE 4. NMR Spectra Data of the Title and Related Complexes at 298 K

Complex	$[Fe_2NiOPH]^a$	$[Fe_2NiOPP]^b$			$[Fe_3OPH]^b$	$[Fe_3OPP]^a$
	δ_H (ppm)	δ_H (ppm)	$\Delta_{1/2}$ (Hz)	T_1 (ms)	δ_H (ppm)	δ_H (ppm)
CH_3 (Fe-Fe)	3.8	4.0	170	3.4	7.4	7.5
CH_3 (Fe-Ni)	4.9	4.4	175	3.3		
CH_2 (Fe-Fe)	9.7	9.9	315	1.9	25.8	25.4
CH_2 (Fe-Ni)	10.6, 10.8	10.7	350	1.9		
2-H (Fe-py)		24.6	2800	0.84		65.0
2-H (Ni-py)		95.4	1265	0.76		
3-H (Fe-py)		11.7	400	3.5		29.0
3-H (Ni-py)		29.2	217	3.7		
4-H (Fe-py)		7.6	205	5.2		8.3
4-H (Ni-py)		14.6	187	5.9		

[a] d_6-DMSO (99.9% dimethyl sulfoxide-d6 with 0.03% V/V TMS). [b] d_3-MeCN.

As shown in Table 4, the chemical shifts of 2-H and 3-H of the pyridine ligands coordinating by Fe^{III} ions in $[Fe_2NiOPP]$ are much smaller than those in $[Fe_3OPP]$. A similar relation exists in the proton chemical shifts of the methylenes of the propionate ligands, which bidentately bridge two Fe^{III} ions. This seems difficult to understand. Prodius et al. [2, 4] found that, compared to $Fe_3^{III}O$ complexes, the mixed-metal $Fe_2^{III}M^{II}O$ (M = Ni, Co, Mn or Mg) complexes revealed a remarkable increase in the strength of the super exchange interaction between two trivalent ions. The super exchange interaction value J_{FeFe} of $[Fe_3^{III}O(O_2CH_3)_6(H_2O)_3]^+$ is –30 cm^{-1} and changes to –73 cm^{-1} for $Fe_2^{III}Ni^{II}O(O_2CC_2H_5)_6(H_2O)_3$ and $Fe_2^{III}Ni^{II}O(O_2CC_2H_5)_6(py)_3$ [4]. This may be due to the asymmetric charge distribution in hetero-trinuclear clusters. The magnetic properties of the complexes provide evidence to support our NMR results. The ^1H chemical shifts of the title complexes in some other common organic solvents such as d_3-MeCN and $CDCl_3$ are similar to the results mentioned above. This means that the complexes are stable in these organic solvents and their skeleton structures in solution are the same as in the solid state. The slight differences of the chemical shifts in these organic solvents come from the solvent effect. However, the ^1H NMR spectrum of $[Fe_2NiOPH]$ in D_2O had only three resonances at 4.8, 2.7, and 1.2, with relative intensities of 2:3 for the latter two peaks. They are readily assigned to the protons of HDO, CH_2 and CH_3, respectively, according to the two resonances of $NaOOCC_2H_5$ in D_2O at 2.34 ppm (CH_2) and 1.22 ppm (CH_3). The ^1H NMR spectrum of $[Fe_2NiOPP]$ in D_2O has three more resonances at ca. 8.8, 8.0, and 8.4 ppm with relative intensities 2:2:1. They are readily assigned to 2-, 3-, and 4-H protons, respectively, because free pyridine in $CDCl_3$ has resonances at 8.50, 7.04, and 7.46 ppm. The small differences in the ^1H chemical shifts between the title complexes and reference compounds may be caused by transition-metal ions and the solvent effect. These experimental results indicate that both the title complexes are not stable in D_2O and decompose into simple hydrated metal ions and corresponding ligands, in agreement with UV experiments. It is worth further studying the mechanism. This may be helpful in guiding synthesis of similar complexes.

Conclusion. In this work, two μ_3-oxo carboxylate-bridged heterotrinuclear complexes $[Fe_2^{III}Ni^{II}O(O_2CC_2H_5)_6(H_2O)_3]\cdot H_2O$ and $[Fe_2^{III}Ni^{II}O(O_2CC_2H_5)_6(py)_3]\cdot py$ were synthesized and characterized by NMR, X-ray diffraction, IR, UV and ESR. XRD results demonstrated that the Fe_2NiO cluster of the complexes is close to threefold symmetry in the crystal. The ligands coordinated to different metal atoms are almost equivalent in the IR timescale but are equivalent in the NMR timescale. Information on the relative intensities, broadening, cross peaks in 2D, spin-lattice relaxation times, substitution effect, etc. was used in the assignments of the ^1H NMR spectra. The solution structures and dynamics of the complexes were studied by variable-temperature ^1H NMR. The main effect on the proton chemical shifts of ligands results from different skeleton metals. NMR experiments showed that the solution structures of the complexes in d_6-DMSO, d_3-MeCN, and $CDCl_3$ solvents are the same as those in the solid state. However, the complexes in water are decomposed into metal ions and the corresponding ligands at room temperature.

Acknowledgment. This work is supported by NNSF of China (81101037).

REFERENCES

1. M. Colmont, O. Mentre, N. Henry, *Prog. J. Solid. State. Chem*., **260**, 101–106 (2018).
2. N. Shan, S. J. Vickers, H. Adams, M. D. Ward, J. A. Thomas, *Angew. Chem. Int. Ed*., **43**, 3938–3943 (2004).
3. I. Ratera, C. Sporer, D. Ruiz-Molina, N. Ventosa, J. Baggerman, A. M. Brouwer, C. Rovira, J. Veciana, *J. Am. Chem. Soc*., **129**, 6117–6121 (2007).
4. A. Olchowka, J. Colmont, M. Aliev, *Cryst. Eng. Commun*., **19**, 936–940 (2017).
5. Xiao-Yu Qi, Kai Wang, Lun Wang, *J. Solid State Chem*., **63**, 91–98 (2016).
6. F. Paul, G. Da Costa, A. Bondon, N. Gauthier, S. Sinbandhit, L. Toupet, K. Costuas, J. F. Halet, C. Lapinte, *Organometallics*, **26**, 874–878 (2007).
7. S. Ghumaan, S. Mukherjee, S. Kar, D. Roy, S. M. Mobin, R. B. Sunoj, G. K. Lahiri, *Eur. J. Inorg. Chem*., **21**, 4426–4430 (2006).
8. D. M. D′Alessandro, F. R. Keene, *Chem. Rev*., **106**, 2270–2276 (2006).
9. R. W. Wu, M. Poyraz, F. E. Sowrey, C. E. Anson, S. Wocadlo, A. K. Powell, U. A. Jayasooriya, R. D. Cannon, T. Nakamoto, M. Katada, H. Sano, *Inorg. Chem*., **37**,1913–1918 (1998).
10. A. Dikhtiarenko, S. Khainakov, J. R. Garcia, *Inorg. Chem*., **454**, 107–122 (2017).
11. S. Kiana, M. Yazdanbakhsh, M. Jamialahmadi, *J. Chem. Soc., Faraday Trans*., **130**, 28–32 (2014).
12. A. Heckmann, C. Lambert, M. Goebel, R. Wortmann, *Angew. Chem. Int. Ed*., **43**, 5851–5855 (2004).
13. N. Suaud, A. Gaita-Arino, J. M. Clemente-Juan, E. Coronado, *Chem. Eur. J*., **10**, 4041–4046 (2004).
14. A. Vlachos, V. Psycharis, C. P. Raptopoulou, N. Lalioti, Y. Sanakis, G. Diamantopoulous, M. Fardis, M. Fardis, M. Karayanni, G. Papavassiliou, A. Terzis, *Inorg. Chim. Acta*, **357**, 3162–3168 (2004).
15. L. Banci, *Nuclear and Electron Relaxation. The Magnetic Nucleus-Unpaired Electron Coupling in Solution*, VCH, Weinheim (1991).
16. J. R. Houston, W. H. Casey, *Inorg. Chem*., **44**, 5176–5122 (2005).
17. M. Itou, M. Otake, Y. Araki, O. Ito, H. Kido, *Inorg. Chem*., **44**, 1580–1586 (2005).
18. M. M. Glass, K. Belmore, J. B. Vincent, *Polyhedron*, **12**, 133–139 (1993).
19. C. P. Raptopoulou, Y. Sanakis, A. K. Boudalis, V. Psycharis, *Polyhedron*, **24**, 711–718 (2005).
20. Z. Chen, S. H. Cai, J. L. Ye, G. T. Lu, L. N. Zhang, *Chin. J. Struct. Chem*., **18**, 227–232 (1999).
21. A. Morsali, S. A. Beyramabadi, H. Chegini, *J. Structural. Chem*., **57**, 875–882 (2016).
22. I. Bertini, Y.K. Gupta, C. Luchinat, G. Parigi, M. Peana, L. Sgheri, J. Yuan, *J. Am. Chem. Soc*., **129**, 12786–12792 (2007).
23. Z. G. Wang, T. R. Holman, L. Que, *Magn. Reson. Chem*., **31**, 78–81 (1993).
24. D. Prodius, C. Turta, V. Mereacre, S. Shova, M. Gdaniec, Y. Simonov, J. Lipkowski, V. Kuncser, G. Filoti, A. Caneschi, *Polyhedron*, **25**, 2175–2182 (2006).
25. I. Khosravi, M. Mirzaei, A. Bauza, *Polyhedron*, **81**, 39–42 (2014).
26. L. Meesuk, U. A. Jayasooriya, R. D. Cannon, *J. Am. Chem. Soc*., **109**, 2009–2012 (1987).
27. M. B. Moreira, C. F. N. Da Silva, R. B. P. Pesci, *Dalton Trans*., **45**, 16799–16803 (2016).
28. Hua-Xin Zhang, Yoichi Sasaki, Masaaki Abe, *J. Org. Chem*., **797**, 29–33 (2015).
29. Minfeng Lu, Marie Colmont, Marielle Huve, *Inorg. Chem*., **53**, 12058–12062 (2014).
30. A. Mavrandonakis, K. Vogiatzis, D. Boese, A. Daniel, *Inorg. Chem*., **54**, 8251–8257 (2015).